Projected single-spin-flip dynamics in the Ising model

A. L. C. Ferreira

Departamento de Física, Universidade de Aveiro, 3810-193 Aveiro, Portugal

Raúl Toral

*Instituto de Física Interdisciplinar y Sistemas Complejos (IFISC), UIB-CSIC, Edificio Mateu Orfila, Campus UIB,
E-07122 Palma de Mallorca, Spain*

We study transition matrices for projected dynamics in the energy-magnetization, magnetization, and energy spaces. Several single-spin-flip dynamics are considered, such as the Glauber and Metropolis canonical ensemble dynamics, and the Metropolis dynamics for three multicanonical ensembles: the flat energy-magnetization, the flat energy, and the flat magnetization histograms. From the numerical diagonalization of the matrices for the projected dynamics we obtain the subdominant eigenvalues and the largest relaxation times for systems of varying size. Although the projected dynamics is an approximation to the full state space dynamics, comparison with some available results, obtained by other authors, shows that projection in the magnetization space is a reasonably accurate method to study the scaling of relaxation times with system size. For each system size, the transition matrices for arbitrary single-spin-flip dynamics are obtained from a single Monte Carlo estimate of the infinite-temperature transition matrix. This makes the method an efficient tool for evaluating the relative performance of any arbitrary local spin-flip dynamics. We also present results for appropriately defined average tunneling times of magnetization and compare their finite-size scaling exponents with results of energy tunneling exponents available for the flat energy histogram multicanonical ensemble.

I. INTRODUCTION

The dynamical critical behavior of statistical physics models is a problem that attracts considerable attention [1–4]. From a fundamental point of view, one is interested in the identification and characterization of the different dynamical universality classes, known to be more restricted than the static ones. Different algorithms for canonical ensemble simulations have been proposed belonging to different universality classes [5,6]. Still, the increasing relaxation times with system size are a major limitation to the statistical precision of the numerical estimates obtained in the simulations. New algorithms, aiming to estimate the number of states of a given energy, have also been proposed [7–9]. These algorithms simulate a multicanonical ensemble with the advantage that a single simulation provides information on the properties of the system in a wide temperature range. However, such algorithms also suffer from slowing down with increasing system size, and the study of their dynamical properties with simple and efficient methods is essential to ascertain their relative performance.

Many numerical methods have been used to study stochastic dynamics of statistical physics models. These methods measure the largest relaxation time of the dynamics, a time that increases with system size according to dynamic finite-size scaling theory. The exact diagonalization of the transition matrix in the full state space can be done only for very small systems. To overcome this limitation, one can instead estimate by Monte Carlo methods the autocorrelation function of the slowest observable in the system, the one whose long-time behavior gives the largest relaxation time. Although this method is free of systematic errors, one needs to consider very long simulation runs to get a reasonably small statistical error in the autocorrelation function. Several

other methods have been used, including a variational technique [3,4] allowing the estimation of the subdominant eigenvalue of the full state space transition matrix.

Projected dynamics was proposed to study metastability and nucleation in the Ising model [10–15]. The idea behind this method is to derive the dynamics in a restricted space of one or several variables. Choosing such variables appropriately and neglecting non-Markovian memory terms, one hopes that the resulting approximated Markovian dynamics is a good approximation to the full state space dynamics. The usefulness of the method has been proved in the context of the study of metastability in the Ising model, where a direct dynamic Monte Carlo simulation is unable to cope with the large time scale of the problem [14]. The nonlumpability of the full state space transition rate matrix with respect to energy and magnetization classification of the states leads to the appearance of memory terms when projecting the dynamics in these restricted spaces [14,16]. To recover the Markovian character of the dynamics, these memory terms are neglected and the resulting projected dynamics becomes only approximated.

In this paper we study the projected dynamics behavior for the square lattice nearest-neighbor Ising model, in the energy and magnetization spaces for two local spin-flip algorithms, namely, the Glauber and the Metropolis *et al.* [17,18] critical canonical ensemble dynamics, and three multicanonical algorithms, the flat energy-magnetization histogram, the flat energy histogram, and the flat magnetization histogram dynamics. Although the dynamics associated with the transition rate matrices in these restricted spaces are only approximate, we show, by comparison with full state space results, that they can be used to get reasonably accurate estimates of the dynamical properties. From the numerical diagonalization of these matrices, and the determination of their sub-

dominant eigenvalue, we compute the largest relaxation times for systems of varying size. The method proposed can be applied to other models and other dynamics, thus leading to a simple and efficient estimation of the scaling with system size of the largest relaxation time. Such studies are needed to assess the relative performance of Monte Carlo simulation algorithms.

Projected dynamics transition rate matrices were also considered in the context of the transition matrix Monte Carlo method [19,20]. Using an acceptance probability written in terms of the infinite-temperature energy space transition matrix, it is possible to perform simulations that visit with equal probability the spectra of energies of the model, thus doing flat energy histogram simulations. For the case of the Ising model that we consider in this work, this algorithm is easily generalized to simulations with a flat energy and magnetization histogram. We use this flat energy-magnetization histogram ensemble to numerically estimate the infinite-temperature transition rate matrix in the space of energy and magnetization from which all the results presented in this work are derived.

For multicanonical algorithms, average tunneling times between the ground state and states with higher energy (for example, zero energy) have been considered [21]. It has been shown that these tunneling times may scale differently with system size when we consider going up (from a low energy to a high energy) or down in energy [22]. We present results, using projected dynamics, for average tunneling times of magnetization in several multicanonical ensembles that show a similar behavior. We compare our results with those of other authors for tunneling times in the energy space.

The method proposed in this paper to study approximately the local dynamics is efficient because (1) the dynamic exponent estimates are reasonably accurate when compared with corresponding quantities obtained by other methods; (2) any arbitrary, single-spin-flip dynamics can be studied from a single Monte Carlo estimation of an infinite-temperature transition matrix in the energy-magnetization space (corresponding to acceptance of all the proposed configurations); the consideration of a specific dynamics comes only from the weighting of this matrix with the corresponding acceptance probability; (3) the dimensional reduction achieved by the projection allows the application of matrix diagonalization techniques for bigger system sizes.

The outline of the paper is as follows. In Sec. II we discuss the projection procedure; in Sec. III we show how the infinite-temperature transition matrix is computed from Monte Carlo simulations for different system sizes and define the projected transition matrices for the different ensembles and dynamics considered. In Sec. IV we present results for the largest relaxation times and the corresponding dynamical exponents. In Sec. V we define and compute tunneling times in the magnetization space and their finite-size scaling exponents, and, finally, in Sec. VI we summarize our main conclusions.

II. PROJECTED DYNAMICS

The Markov chain master equation in the full state space is

$$\frac{dP(\vec{\sigma},t)}{dt} = \sum_{\vec{\sigma}'} [W(\vec{\sigma},\vec{\sigma}')P(\vec{\sigma}',t) - P(\vec{\sigma},t)W(\vec{\sigma}',\vec{\sigma})], \quad (1)$$

where $\vec{\sigma}$ denotes a state of the system, $P(\vec{\sigma},t)$ is the probability for the system to be in a given state at time t, and $W(\vec{\sigma},\vec{\sigma}')$ is the transition rate from state $\vec{\sigma}'$ to $\vec{\sigma}$. In the case of an Ising model $\vec{\sigma} \equiv (\sigma_1,\dots,\sigma_N)$ specifies the state of each of N spins of the system, σ_i, which can take two values, $\sigma_i = \pm 1$. The transition rate obeys detailed balance,

$$P_{st}(\vec{\sigma})W(\vec{\sigma}',\vec{\sigma}) = P_{st}(\vec{\sigma}')W(\vec{\sigma},\vec{\sigma}'), \quad (2)$$

relative to a stationary distribution $P_{st}(\vec{\sigma})$, which we consider to be an arbitrary function $P_{st}(E(\vec{\sigma}),M(\vec{\sigma}))$, of the energy $E(\vec{\sigma}) = -\sum_{\langle i,j \rangle} \sigma_i \sigma_j$ (where the sum is over all neighbor pairs $\langle i,j \rangle$), and the magnetization $M(\vec{\sigma}) = \sum_i \sigma_i$.

The detailed balance equation can be summed for all $\vec{\sigma}$ states with a given energy $E = E(\vec{\sigma})$ and magnetization $M = M(\vec{\sigma})$, and all $\vec{\sigma}'$ states with energy $E' = E(\vec{\sigma}')$ and magnetization $M' = M(\vec{\sigma}')$, to obtain

$$\sum_{\vec{\sigma},\vec{\sigma}'} P_{st}(\vec{\sigma})W(\vec{\sigma}',\vec{\sigma})\delta_{E,E(\vec{\sigma})}\delta_{E',E(\vec{\sigma}')}\delta_{M,M(\vec{\sigma})}\delta_{M',M(\vec{\sigma}')}$$

$$= \sum_{\vec{\sigma},\vec{\sigma}'} P_{st}(\vec{\sigma}')W(\vec{\sigma},\vec{\sigma}')\delta_{E,E(\vec{\sigma})}\delta_{E',E(\vec{\sigma}')}\delta_{M,M(\vec{\sigma})}\delta_{M',M(\vec{\sigma}')},$$

$$(3)$$

$\delta_{a,b}$ being the Kronecker delta. Since the stationary distribution is assumed to be a function of the energy and magnetization only, it can be taken out of the summation, giving

$$p(E,M)T(E',M';E,M) = p(E',M')T(E,M;E',M'), \quad (4)$$

where $p(E,M)$ is the stationary probability for a macrostate characterized by an energy E and a magnetization M, obtained by multiplying the corresponding microstate probability $P_{st}(E,M)$ by $\Omega(E,M)$, the number of states with energy E and magnetization M. In this expression, we have defined

$$T(E',M';E,M)$$

$$= \frac{1}{\Omega(E,M)} \sum_{\vec{\sigma},\vec{\sigma}'} W(\vec{\sigma}',\vec{\sigma})\delta_{E,E(\vec{\sigma})}\delta_{E',E(\vec{\sigma}')}\delta_{M,M(\vec{\sigma})}\delta_{M',M(\vec{\sigma}')}$$

$$(5)$$

as the transition matrix between energy and magnetization states (E,M) and (E',M').

Summing the master equation in the same way we would obtain the evolution equation for the time-dependent probability $p(E,M,t)$ for the system to have energy E and magnetization M at time t:

$$\frac{dp(E,M,t)}{dt} = \sum_{E',M'} [T(E,M;E',M';t)p(E',M',t)$$

$$- p(E,M,t)T(E',M';E,M;t)], \quad (6)$$

with a time-dependent transition matrix

$$T(E',M';E,M;t)$$

$$= \frac{1}{p(E,M,t)} \sum_{\vec{\sigma},\vec{\sigma}'} P(\vec{\sigma},t) W(\vec{\sigma}',\vec{\sigma}) \delta_{E,E(\vec{\sigma})} \delta_{E',E(\vec{\sigma}')}$$

$$\times \delta_{M,M(\vec{\sigma})} \delta_{M',M(\vec{\sigma}')}. \qquad (7)$$

This time-dependent matrix approaches the transition rate matrix in Eq. (5) for large times when $P(\vec{\sigma},t)/p(E,M,t) \rightarrow 1/\Omega(E,M)$. The so-called projected dynamics neglects this time dependence and considers instead the Markov process associated with $T(E',M';E,M)$:

$$\frac{dp(E,M,t)}{dt} = \sum_{E',M'} [T(E,M;E',M')p(E',M',t)$$

$$- p(E,M,t)T(E',M';E,M)]. \qquad (8)$$

Starting with the projection operator technique, in a discrete time formulation, the approximation can be regarded as equivalent to dropping out some memory terms [12]. Note that the dynamics of the Markovian process associated with these transition matrices would be equivalent to the full state space dynamics if it were lumpable [16] with respect to a classification of the states in terms of energy and magnetization. However, this is known not to be the case for canonical ensemble dynamics [14], although the flat magnetization ensemble that we study later is lumpable with respect to a magnetization classification of the states.

Further projection on the energy space can be done by summing for all M and M' the detailed balance condition in the E,M space [Eq. (4)]:

$$p(E) \sum_{M,M'} \frac{p(E,M)}{p(E)} T(E',M';E,M)$$

$$= p(E') \sum_{M,M'} \frac{p(E',M')}{p(E')} T(E,M;E',M'), \qquad (9)$$

which is a detailed balance relation $p(E)T(E';E) = p(E')T(E;E')$ in the energy space with a projected transition matrix

$$T(E';E) = \sum_{M,M'} \frac{p(E,M)}{p(E)} T(E',M';E,M). \qquad (10)$$

Note that for the ensembles where $P_{st}(\vec{\sigma})$ depends just on the energy (and not on the magnetization) the previous expression can be simplified to

$$T(E';E) = \frac{1}{\Omega(E)} \sum_{M,M'} \Omega(E,M)T(E',M';E,M)$$

$$= \frac{1}{\Omega(E)} \sum_{\vec{\sigma},\vec{\sigma}'} W(\vec{\sigma}',\vec{\sigma}) \delta_{E,E(\vec{\sigma})} \delta_{E',E(\vec{\sigma}')}, \qquad (11)$$

where $\Omega(E) = \Sigma_M \Omega(E,M)$ is the number of states with energy E. If $P_{st}(\vec{\sigma})$ depends on energy and magnetization simultaneously, the above simplification cannot be made.

The transition matrix $T(E;E')$ can be used to define a Markov chain dynamics in the restricted energy space:

$$\frac{dp(E,t)}{dt} = \sum_{E'} [T(E;E')p(E',t) - p(E,t)T(E';E)]. \qquad (12)$$

In the same way we can obtain a detailed balance relation in the magnetization space:

$$p(M) \sum_{E,E'} \frac{p(E,M)}{p(M)} T(E',M';E,M)$$

$$= p(M') \sum_{E,E'} \frac{p(E',M')}{p(M')} T(E,M;E',M'), \qquad (13)$$

which is a detailed balance relation $p(M)T(M';M) = p(M')T(M;M')$ in the magnetization space with a projected transition matrix

$$T(M';M) = \sum_{E,E'} \frac{p(E,M)}{p(M)} T(E',M';E,M). \qquad (14)$$

The transition matrix $T(M;M')$ can be used to define a Markov chain dynamics in the restricted magnetization space:

$$\frac{dp(M,t)}{dt} = \sum_{M'} [T(M;M')p(M',t) - p(M,t)T(M';M)].$$

$$(15)$$

Regardless of the approximation assumed in the projected dynamics, the detailed balance relations satisfied by the transition matrices defined above assure that the long-time behaviors of the related stochastic processes defined by Eqs. (8), (12), and (15) are still characterized by the correct stationary probability distributions $p(E,M)$, $p(E)$, and $p(M)$, respectively.

In the following sections, we study single-spin-flip dynamics in the canonical ensemble characterized by the stationary distribution at inverse temperature β, $P_{st}(\vec{\sigma}) = \exp[-\beta E(\vec{\sigma})]/Z$ as well as three multicanonical ensembles with flat energy-magnetization, flat energy, and flat magnetization histograms with $P_{st}(\vec{\sigma}) = 1/\Omega(E,M)$, $P_{st}(\vec{\sigma}) = 1/\Omega(E)$, and $P_{st}(\vec{\sigma}) = 1/\Omega(M)$, respectively. Note that $\Omega(M) = \Sigma_E \Omega(E,M)$ is exactly known to be

$$\Omega(M) = \binom{N}{\frac{N+M}{2}}$$

and that an efficient numerical scheme (not used by us in the present work) developed by Beale [23] allows exact computation of $\Omega(E)$ for the two-dimensional Ising model for moderate system sizes N. The number of states $\Omega(E,M)$ for the two-dimensional Ising model was also numerically calculated before by using an entropic sampling method and the broad-histogram method [11,24]. We are not aware of previous studies concerning the flat magnetization ensemble studied in the present work.

III. NUMERICAL CALCULATION OF TRANSITION MATRICES

We now explain our method to compute numerically the transition matrices $T(E',M';E,M)$, $T(E';E)$, and $T(M';M)$ defined in Eqs. (5), (10), and (14), respectively. We start by recalling that for single-spin-flip dynamics the transition rate $W(\vec{\sigma}',\vec{\sigma})$ can be separated into a proposal step and an acceptance step. In the proposal step we choose, with equal probability, one of the spins of the system and propose to flip it. Thus a given system state may have a nonzero transition rate to N other system states that differ in the state of a single spin. In the acceptance step we accept the proposed configuration with a probability $a(E',M';E,M)$ that we assume depends only on the energy and magnetization of the initial and final configurations.

Consider the detailed balance relation (4) when we sample with equal probability all the states of the system. This is the case, for example, of the canonical ensemble Metropolis *et al.* algorithm at infinite temperature when we accept all the proposed configurations. The probability to measure an energy E and magnetization M is then equal to $\Omega(E,M)/2^N$ since all states have equal probability. Thus we can write the relation

$$\Omega(E,M)T_\infty(E',M';E,M) = \Omega(E',M')T_\infty(E,M;E',M'),$$
(16)

known as the broad-histogram equation [25,26]. For a general single-spin-flip algorithm characterized by $a(E',M';E,M)$, we can write

$$T(E',M';E,M) = T_\infty(E',M';E,M)a(E',M';E,M),$$
(17)

with $T_\infty(E',M';E,M)=\langle N(\vec{\sigma},\Delta E,\Delta M)\rangle_{E,M}/N$ the normalized average, in the constant energy and magnetization ensemble, of the number of configurations $N(\vec{\sigma},\Delta E,\Delta M)$ with energy $E'=E+\Delta E$ and magnetization $M'=M+\Delta M$ that can be obtained from configuration $\vec{\sigma}$ by flipping a single spin. The idea of calculating the microcanonical average of the number of possible updates from a state of energy E to a state of energy E' was first introduced in [25,26]. It was later shown [27] that, for an arbitrary reversible procedure for updating a configuration (a proposal), not necessarily one that updates a single spin, an equation similar to Eq. (16) is always satisfied by the microcanonical average $\langle N(\vec{\sigma},\Delta E)\rangle_E$, interpreted, more generally, as the average of the number of possible ways (independently of the proposal probabilities) of changing the state of the system from one with energy E to another with energy $E'=E+\Delta E$.

The numerical determination of $T_\infty(E',M';E,M)$ can be done from the estimator

$$T_\infty(E',M';E,M)$$
$$= \frac{1}{NH_{sim}(E,M)}\sum_{k=1}^{N_m} N(\vec{\sigma}_k,\Delta E,\Delta M)\delta_{E,E(\vec{\sigma}_k)}\delta_{M,M(\vec{\sigma}_k)},$$
(18)

where the summation is done over the N_m configurations

generated by the Monte Carlo procedure. $H_{sim}(E,M)$ is the energy and magnetization histogram of the simulation. It can be seen that this is the correct estimator, whatever the simulation ensemble [27] we are using, by considering that

$$\langle N(\vec{\sigma},\Delta E,\Delta M)\rangle_{E,M}$$
$$= \frac{1}{\Omega(E,M)}\sum_{\vec{\sigma}} N(\vec{\sigma},\Delta E,\Delta M)\delta_{E,E(\vec{\sigma})}\delta_{M,M(\vec{\sigma})}$$
$$= \left\langle \frac{N(\vec{\sigma},\Delta E,\Delta M)\delta_{E,E(\vec{\sigma})}\delta_{M,M(\vec{\sigma})}}{P_{sim}(\vec{\sigma})\Omega(E,M)} \right\rangle_{sim},$$
(19)

where $P_{sim}(\vec{\sigma})$ is the probability of visiting a particular state in the simulation ensemble whose averages are denoted by $\langle\cdots\rangle_{sim}$, and noting that $H_{sim}(E,M)=N_m P_{sim}(\vec{\sigma})\Omega(E,M)$ with $P_{sim}(\vec{\sigma})$ dependent only on E and M.

For the two-dimensional square lattice nearest-neighbor Ising model, each spin can have between zero and four nearest neighbors in the same state of the spin. When this spin flips there are five possible energy changes ΔE, and two magnetization changes ΔM. Thus, one needs to count the number of spin flips that lead to an energy and magnetization change in each of these possible ten classes.

In this work we have estimated $T_\infty(E',M';E,M)$ by doing transition matrix Monte Carlo simulations in the above-mentioned Ising model of size $N=L^2$ with an acceptance probability $a(E',M';E,M)=\min\left(1,\frac{T_\infty(E,M;E',M')}{T_\infty(E',M';E,M)}\right)$. From Eqs. (4) and (17) we can see that this choice leads to a flat energy and magnetization histogram. The algorithm starts with an initial estimate of $T_\infty(E',M';E,M)$ that is improved as more configurations are generated. We have used the n-fold way simulation algorithm of Kalos and Lebowitz [20,28], and the number of simulated spin flips per number of spins was 10^8 for each of the systems studied, $L=3,\ldots,21,30$. Note that, when one considers an n-fold way simulation, the histogram of energy and magnetization, $H_{sim}(E,M)$, is the average time spent at a given value of energy and magnetization. This may differ from the average number of hits to a particular energy and magnetization value. In this case, the expression (18) should be modified to weight each of the generated configurations with the estimated average time spent in these configurations (a small but systematic error arises in the results if this weighting is not done).

The projected transition matrices in the energy-magnetization space, $T(E',M';E,M)$, are obtained from the simulation estimates of $T_\infty(E',M';E,M)$ by using Eq. (17). We consider the following dynamics: (1) the Metropolis canonical ensemble dynamics with $a(E',M';E,M)=\min(1,\exp[-\beta(E'-E)])$; (2) the Glauber canonical ensemble dynamics with $a(E',M';E,M)=\frac{1}{2}\{1-\tanh[\frac{\beta}{2}(E'-E)]\}$; (3) the flat energy and magnetization histogram Metropolis dynamics with $a(E',M';E,M)=\min\left(1,\frac{T_\infty(E,M;E',M')}{T_\infty(E',M';E,M)}\right)$; (4) the Metropolis flat energy dynamics (also known as entropic sampling) with $a(E',M';E,M)$

$=\min\left(1,\dfrac{\Omega(E)}{\Omega(E')}\right)$; and (5) the Metropolis flat magnetization dynamics with $a(E',M';E,M)=\min\left(1,\dfrac{\Omega(M)}{\Omega(M')}\right)$.

For the energy-magnetization space with dimension $(N+1)^2\times(N+1)^2$, we have obtained results from the diagonalization of $T(E',M';E,M)$ up to $N=8^2$. For all the system sizes studied we have found the stationary probabilities $p(E,M)$ after solving numerically the system of equations Eq. (8) in the steady state regime:[1]

$$\sum_{E',M'}[T(E,M;E',M')p(E',M')-p(E,M)T(E',M';E,M)]$$
$$=0. \qquad (20)$$

For the flat energy histogram dynamics we need to know $\Omega(E)$ to construct the corresponding acceptance probability. This quantity can be obtained from $\Omega(E,M)$ after the solution of the homogeneous linear system of equations

$$\sum_{E',M'}[T_\infty(E,M;E',M')\Omega(E',M')$$
$$-\Omega(E,M)T_\infty(E',M';E,M)]=0. \qquad (21)$$

Note that it is possible to compute

$$T_\infty(E';E)=\sum_{M',M}\frac{\Omega(E,M)}{\Omega(E)}T_\infty(E',M';E,M), \qquad (22)$$

and write $a(E',M';E,M)=\min\left(1,\dfrac{T_\infty(E;E')}{T_\infty(E';E)}\right)$ for a flat energy histogram ensemble which is completely equivalent to $a(E',M';E,M)=\min\left(1,\dfrac{\Omega(E)}{\Omega(E')}\right)$.

IV. LARGEST RELAXATION TIMES

We have considered a discrete time transition matrix defined as $\gamma(E,M;E'M')=T(E,M;E'M')$ for $(E,M)\neq(E',M')$ and $\gamma(E,M;E,M)=1-\sum_{E',M'}T(E',M';E,M)$ for $(E,M)\equiv(E',M')$. This corresponds to the Markov chain equation $p(E,M,t+1)=\sum_{E',M'}\gamma(E,M;E'M')p(E',M',t)$. The stationary probability distribution corresponds to an eigenvector with the largest eigenvalue 1. The second largest eigenvalue, λ, determines the largest relaxation time in the system, $\tau=-1/N\ln\lambda$. The division by N is needed in order for τ to be expressed in units of numbers of Monte Carlo steps per total number of spins. The relaxation times increase with system size as $\tau\sim L^z$, thus being characterized by a dynamic exponent z.

We have studied the behavior of the projected dynamics at the critical point of the square lattice Ising model, $\beta_c J$

TABLE I. Subdominant eigenvalues of transition matrices for different system sides L and Glauber dynamics. The second column lists values for the matrix $W(\vec{\sigma},\vec{\sigma}')$ taken from Refs. [3,4]. The third and fourth columns are our results for the matrices $T(M;M')$ and $T(E,M;E'M')$, respectively.

L	λ^W, Refs. [3,4]	$\lambda^{T(M;M')}$	$\lambda^{T(E,M;E',M')}$
3	0.997409385126011[a]	0.9973901755	0.99740630184576[a]
			0.9974063007
4	0.999245567376453[a]	0.9992429803	0.99924409354918[a]
			0.9992441209
5	0.999708953624452[a]	0.9997066202	0.99970673172786[a]
			0.9997067351
6	0.9998657194	0.9998635780	0.9998637800
7	0.9999299708	0.9999281870	0.9999284453
8	0.9999600854	0.9999586566	0.9999589090
9	0.9999756630	0.9999744986	
10	0.9999843577	0.9999834244	
11	0.9999895056	0.9999887396	
12	0.9999927107	0.9999921039	
13	0.9999947840	0.9999942741	
14	0.9999961736	0.9999957520	
15	0.9999971315	0.9999967823	
16	0.9999978080	0.9999975119	
17	0.9999982987	0.9999980505	
18	0.9999986606	0.9999984474	
19	0.9999989315	0.9999987550	
20	0.9999991370	0.9999989750	
21	0.9999992955	0.9999991723	
30		0.9999998016	

[a]Exact: λ^W from diagonalization of the full state matrix W and $\lambda^{T(E,M;E',M')}$ obtained from diagonalization of the exact projection matrix $T(E,M;E',M')$ obtained from the enumeration of all the states.

$=\frac{1}{2}\ln(1+\sqrt{2})$, for canonical Glauber and Metropolis *et al.* acceptance probabilities. For Glauber dynamics, the eigenvalue results $\lambda^{T(M;M')}$ from the matrix $T(M;M')$, and $\lambda^{T(E,M;E'M')}$ from $T(E,M;E'M')$ can be seen in Table I together with the eigenvalues λ^W for the full state space dynamics obtained from [3,4] using a variational method. For small systems $L=3,4,5$ we have also computed $\lambda^{T(E,M;E'M')}$ from an exact enumeration of all the system states and the results are in close agreement with the ones obtained from the Monte Carlo estimation of $T_\infty(E,M;E',M')$. For a given system side L, the eigenvalues are close to each other and are observed to obey the inequality $\lambda^W>\lambda^{T(E,M;E'M')}>\lambda^{T(M;M')}$ which may be regarded, variationally, as a consequence of not being possible to write the exact full state eigenvector as a function only of energy and magnetization. An estimate of the error in the $\lambda^{T(M;M')}$ values in Table I, for $L=15$, was obtained by making ten simulations of 10^7 Monte Carlo steps MCS/spin giving $\Delta\lambda=8\times10^{-9}$ corresponding to a relative error of 2.5×10^{-3} in the correlation time.

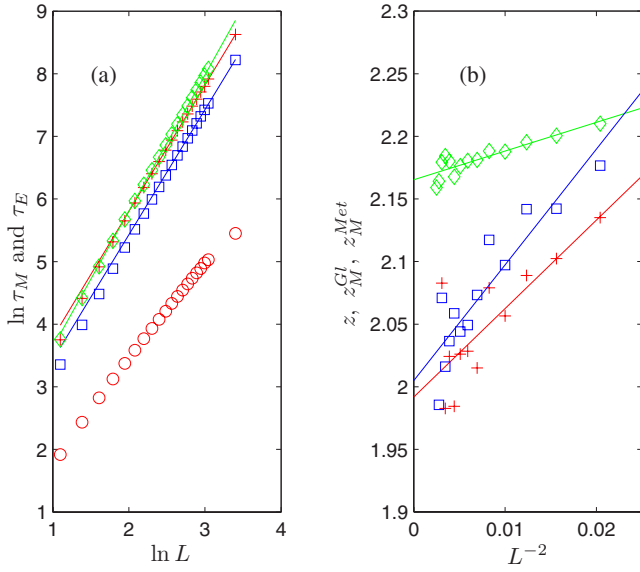In Fig. 1(a) we plot on a log-log scale the dependence with system size L of the magnetization relaxation times, τ_M^{Gl}

---

[1]The solution has been found by an iterative method in which, at each iteration, the values of the energy-magnetization probability at (E_1,M_1) and $(E_1,-M_1)$ are kept constant with a value $p(E_1,M_1)=p(E_1,-M_1)=1/2$. This procedure was found to improve the convergence considerably. The values of (E_1,M_1) were chosen to be near the (E,M) region where $p(E,M)$ has an appreciable value. The iteration was stopped when the measured relative change of $\sum_{E,M}p(E,M)$ was smaller than 10^{-12}.

FIG. 1. (Color online) (a) Relaxation times τ_M for Glauber dynamics obtained from Ref. [4] ($\diamond$) and from the subdominant eigenvalue of the matrix $T(M;M')$ (+). In the latter case, we also plot the corresponding values for the canonical Metropolis *et al.* dynamics ($\square$). The fitted straight lines to the log-log plot were obtained neglecting data for $L<15$ and have slopes $z=2.18$, $z_M^{Gl}=2.02$, and $z_M^{Met}=2.00$. The graph also displays the energy relaxation time τ_E^{Gl} for Glauber dynamics obtained from the matrix $T(E;E')$ ($\bigcirc$). In this case, the observed behavior is $\tau_E^{Gl} \sim \ln L$. (b) Estimations of the dynamic critical exponent from the local slopes of the graph in (a) as a function of L^{-2}. The symbols are as in (a). The extrapolated exponents are $z_M^{Gl}=1.99(2)$, $z_M^{Met}=2.01(1)$, and $z=2.165(3)$.

of the critical canonical Glauber dynamics and τ_M^{Met} of the Metropolis *et al.* dynamics, obtained from the subdominant eigenvalue of $T(M;M')$, together with the full state space values τ of [3,4]. In this graph, the fitted straight lines were obtained neglecting data for $L<15$ and have slopes $z_M^{Gl}=2.02$, $z_M^{Met}=2.00$, and $z=2.18$. However, to obtain a more reliable estimate of the exponents z, a careful analysis taking into account corrections to scaling is needed. We have considered the first-order finite-size correction to the leading behavior [3,4], $\tau \sim L^z(1+bL^{-2})$, by plotting in Fig. 1(b) the local slope $z=\ln[\tau(L+1)/\tau(L)]/\ln[(L+1)/L]$ as a function of L^{-2}. The extrapolation to infinite system size limit yields $z_M^{Gl}=1.99(2)$, $z_M^{Met}=2.01(1)$, and $z=2.165(3)$. The estimated error bars for the exponents, quoted in this work, correspond to fitting probabilities [29] equal to 1. The results for z_M^{Gl} and z_M^{Met} seem to be compatible with $z_M^{Gl}=z_M^{Met}=2$, while the result for z is consistent with the best estimate of Ref. [4], $z=2.1660(10)$, thus excluding the Domany conjecture $z=2$ with a logarithmic correction $\tau \sim L^2(1+b\ln L)$ [30], although further analysis [31] of the same data was not able to categorically exclude the validity of the Domany conjecture.

In Fig. 1(a) we also plot the energy relaxation time τ_E^{Gl} for the critical canonical Glauber dynamics, obtained from the subdominant eigenvalue of matrix $T(E;E')$. Note that we use now a linear scale in the vertical axis and hence the observed behavior is $\tau_E^{Gl} \sim \ln L$. This logarithmic behavior is indicated
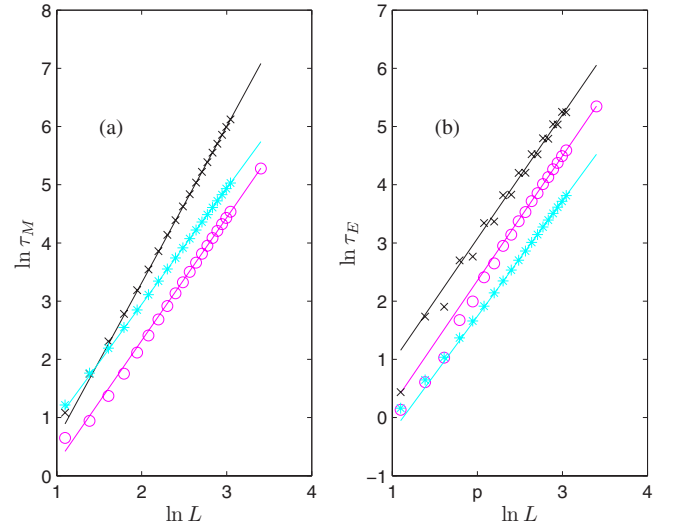

FIG. 2. (Color online) Relaxation times obtained for the Metropolis *et al.* dynamics in the flat energy-magnetization ensemble ($\bigcirc$), flat magnetization ensemble ($*$), and flat energy ensemble ($\times$). In (a) we plot the magnetization relaxation times τ_M obtained from $T(M;M')$, and the fitted straight lines have slopes $z_M^{E-M}=2.11$, $z_M^E=2.69$, and $z_M^M=1.99$. In (b) we plot the energy relaxation times τ_E obtained from $T(E;E')$, and the fitted straight lines have slopes $z_E^{E-M}=2.14$, $z_E^E=2.13$, and $z_E^M=1.99$. In both (a) and (b) data for $L<15$ were neglected in the fits.

by a critical exponent $z_E^{Gl}=0(\log)$, in accordance with previously reported results [19].

In Fig. 2(a) we plot the magnetization relaxation times obtained from $T(M;M')$ for the Metropolis *et al.* dynamics in the flat energy-magnetization ensemble, τ_M^{E-M}, the flat energy ensemble, τ_M^E, and the flat magnetization ensemble, τ_M^M. The fitted straight lines (excluding again data for $L<15$) in the log-log plot have slopes $z_M^E=2.69$, $z_M^M=1.99$, and $z_M^{E-M}=2.11$. As before, better estimates of these exponents, including correction to scaling terms, are obtained from extrapolation to the infinite-size limit of the local slopes. The analysis, performed in Fig. 3(a), yields $z_M^E=2.68(3)$, $z_M^M=1.9995(5)$, and $z_M^{E-M}=2.08(1)$. The value for z_M^E is compatible with the available [32] result $z=2.80(13)$ obtained by a Monte Carlo estimate of the convergence time of the time-dependent energy histogram to the stationary flat distribution of the energy. The data for z_M^{E-M} show an even-odd effect, and it is important to do separate estimates for even and odd system sides.

Note that the full state transition rate matrix W, in the flat magnetization ensemble, is lumpable with respect to the classification of the states according to their magnetization and, consequently, the result $z_M^M \sim 2$ does not suffer from the approximation inherent in the projection procedure. A sufficient and necessary condition for lumpability [16] is that the total probability to go from a state belonging to a given magnetization class to another class with different magnetization is the same for every state in the starting class. For each state in the starting class with magnetization M there are $n_\pm$ states in the final class $M\pm2$ where $n_\pm$ is the number of up (down) spins in the initial configuration. The probability to move to each of these final states in the final class has a constant
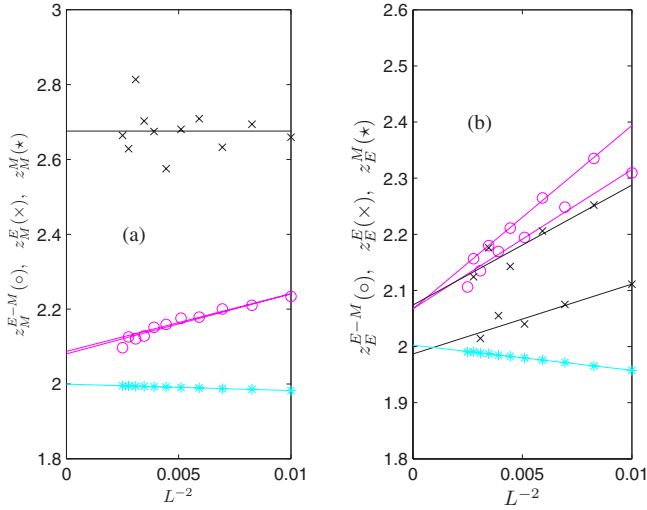
FIG. 3. (Color online) (a) Dynamic exponent estimates z_M^{E-M} (○), z_M^E (×), and z_M^M (∗) from local slopes of the plots shown in Fig. 2(a) as a function of L^{-2}. For the estimates for the energy-magnetization flat multicanonical ensemble, we made separate estimations for even and odd L system sides. The infinite system size extrapolations give $z_M^{E-M} = 2.08(1)$, $z_M^E = 2.68(3)$, and $z_M^M = 1.9995(5)$. (b) Dynamic exponent estimates z_E^{E-M} (○), z_E^E (×), and z_E^M (∗) from local slopes of the plots shown in Fig. 2(b) as a function of L^{-2}. For the magnetization flat multicanonical ensemble, the result is $z_E^M = 2.002(1)$. For the energy-magnetization flat multicanonical ensemble, the separate even and odd L system sides estimates coincide and give $z_E^{E-M} = 2.07(1)$. For the flat energy ensemble, extrapolations from odd and even size yield $z_E^E = 2.07(3)$ and $1.99(2)$, respectively.

value that depends only on the initial M and on the final $M \pm 2$. All the states in the starting class have the same number of up spins and down spins, so the probability to move to $M \pm 2$ is the same for every state in the starting class. The matrix $T(M;M')$ is a tridiagonal symmetric matrix with matrix elements given by $T(M+2;M) = T(M;M+2) = (1+n_+)/N$ for $M<0$, and $T(M+2;M) = T(M;M+2) = n_-/N$ for $M \geq 0$.

Finally, in Fig. 2(b) we plot the energy relaxation times obtained from $T(E;E')$ for the Metropolis *et al.* dynamics in the same ensembles as in the case of the magnetization. The slopes of the fitted straight lines (again excluding $L<15$) are $z_E^{E-M} = 2.14$, $z_E^E = 2.13$, and $z_E^M = 1.99$. The more detailed analysis taking into account correction to scaling terms, shown in Fig. 3(b), yields $z_M^E = 2.002(1)$. In the case of z_E^{E-M}, odd and even side extrapolations are very close to each other and give $z_E^{E-M} = 2.07(1)$. However, the extrapolations for z_E^E for odd and even system sides differ, giving $z_E^E = 2.07(3)$ and $z_E^E = 1.99(2)$, respectively. The difference between these two estimates may be a sign of the presence of corrections to scaling not properly accounted for by our analysis.

V. MAGNETIZATION TUNNELING TIMES

As a measure of performance for multicanonical methods, the average tunneling times were introduced [21]. These tunneling times measure the time required to sample the whole

phase space and scale with system size differently from the relaxation time. It was shown that it is important to distinguish between tunneling from the ground state to maximum energy, the up direction, and from high energy to the ground state, the down direction [22].

All the tunneling times reported by us are calculated for the projected dynamics associated with $T(M;M')$. We calculate the average time τ_t for the system to go from magnetization $M=-N$ to $M=N$. We also consider two other average times: the time τ_u for the system to go from $M=-N$ to zero magnetization, and the time τ_d for the system to go either to $M=+N$ or $M=-N$ when it starts from $M=0$. The definitions of τ_u and τ_d apply only to systems with even L (and N), such that $M=0$ is an accessible value of the magnetization.

The tunneling times defined above obey the relation $\tau_u + \tau_d = \tau_t/2$ which follows from the following simple argument. For the system to go from $M=-N$ to $M=N$ it has to reach $M=0$ at some point. It will do so for the first time using an average time τ_u. Then with probability $1/2$ it will reach for the first time $M=N$ and the tunneling time will be $\tau_u + \tau_d$, or it will return to $M=-N$ and it will reach $M=N$ later, taking a time $\tau_u + \tau_d + \tau_t$. Consequently the tunneling times obey the relation $\frac{1}{2}(\tau_u + \tau_d) + \frac{1}{2}(\tau_u + \tau_d + \tau_t) = \tau_t$. This argument uses the fact that the matrix $T(M;M')$ has the symmetry property $T(M \pm 2;M) = T(-M \mp 2;-M)$, and so the walk along positive values of the magnetization has the same statistical properties as the walk along negative values of the magnetization.

The time to go from $M=-N$ to $M=N$ can be easily computed by taking advantage of the fact that $T(M;M')$ is non-zero only when $M=M' \pm 2$ and $M'=M$. If we do not allow transitions from $M=N$ to $M=N-2$, $M=N$ becomes an absorbing site for every walk along the magnetization axis, meaning that it will end there upon a first visit. Defining $h(M)$ as the average time spent at magnetization value M [14], we can write

$$h(M-2)T(M;M-2) - h(M)T(M-2;M) = 1, \quad (23)$$

which means that the difference between the average number of jumps in the positive direction ($M-2 \rightarrow M$) and the average number of jumps in the negative direction ($M \rightarrow M-2$) should be equal to 1 since the system will eventually reach $M=N$ by moving one time in excess in the positive direction through the bond connecting the sites $M-2$ and M. At $M=N$ there are no jumps in the negative direction and so $h(N-2)T(N;N-2) = 1$. It is then simple to calculate $h(M)$ and the average tunneling time for the system to go from $M=-N$ to $M=N$ is given by $\tau_t = \sum_{M=-N}^{M=N-2} h(M)$.

The time τ_u to reach for the first time $M=0$ starting from $M=-N$ is obtained using the recursion (23) together with the equation $h(-2)T(0;-2) = 1$ to get $\tau_u = \sum_{M=-N}^{M=-2} h(M)$. Finally, the average time required to start from $M=0$ and reach for the first time either $M=-N$ or $M=N$, τ_d, is obtained from the recursion

$$h(M)T(M-2;M) - h(M-2)T(M;M-2) = 1 \quad (24)$$

with a modified rate $T(-2;0)$ equal to $T(-2;0) + T(2;0)$ and $h(-N+2)T(-N;-N+2) = 1$. The average time τ_d is then given
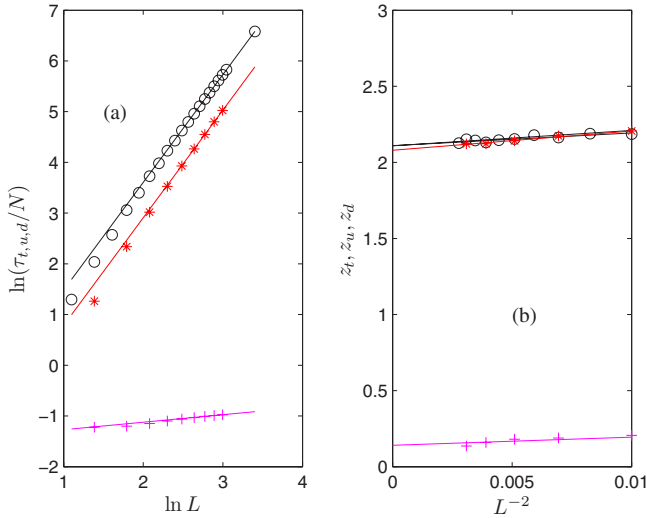
FIG. 4. (Color online) (a) Tunneling times τ_t ($\bigcirc$), τ_u (+), and τ_d (*) as a function of system size L for the Metropolis *et al.* dynamics in a flat magnetization-energy histogram ensemble obtained from the matrix $T(M;M')$. The fitted straight lines were obtained neglecting data for $L<15$ and have slopes $z_t=2.12$, $z_u=0.15$, and $z_d=2.12$, respectively. In (b) we plot the corresponding local slopes as a function of L^{-2}. Even and odd system sides were treated separately. The infinite-system extrapolation gives $z_t=2.11(1)$, $z_u=0.14(2)$, and $z_d=2.08(1)$.

by $\tau_d=\sum_{M=-N+2}^{M=0}h(M)$. The average tunneling times obtained by this method could also have been obtained from the calculation of the probability of the first visit to the absorbing site that can be computed from the eigenstates and eigenvectors of the associated absorbing Markov chain matrix (see [22]).

The tunneling times are characterized by dynamic exponents [21], $\tau_t\sim L^{d+z_t}$, $\tau_u\sim L^{d+z_u}$, $\tau_d\sim L^{d+z_d}$. The relation between these tunneling times implies that z_t is equal to the biggest of the two exponents, z_u and z_d, $z_t=\max(z_d,z_u)$. Note that the tunneling times reported by us are measured in units of lattice sweeps and not in units of site updates.

In Fig. 4(a) we show the size dependence of the tunneling times τ_t, τ_u, and τ_d for the Metropolis *et al.* dynamics in a flat magnetization-energy histogram ensemble obtained from the matrix $T(M;M')$. We see that $\tau_t\sim\tau_d\gg\tau_u$. A direct fit to the log-log plot gives scaling exponents $z_u=0.15$, $z_t=z_d=2.12$. Note that for a random walk on the magnetization axis a value for these exponents equal to 0 is expected. The corrections to scaling terms are analyzed in Fig. 4(b) where we show the local slopes for the plots in Fig. 4(a) as a function of L^{-2}. The estimates for z_t and z_d seem to follow a straight line predicting an infinite system value 2.11(1) and 2.08(1), respectively. The infinite-size extrapolation for z_u is 0.14(2), which predicts a scaling $\tau_u\sim L^{2.14}$ close to the exponent of the relaxation time $z_M^{E-M}=2.08$ reported in the previous section. This behavior is similar to the one found in [22] where τ_u (in the energy space) was found to scale like the relaxation time of the system.

In Fig. 5(a) we show the size dependence of the tunneling times τ_t, τ_u, and τ_d for the Metropolis *et al.* dynamics in a flat energy histogram ensemble obtained from the matrix
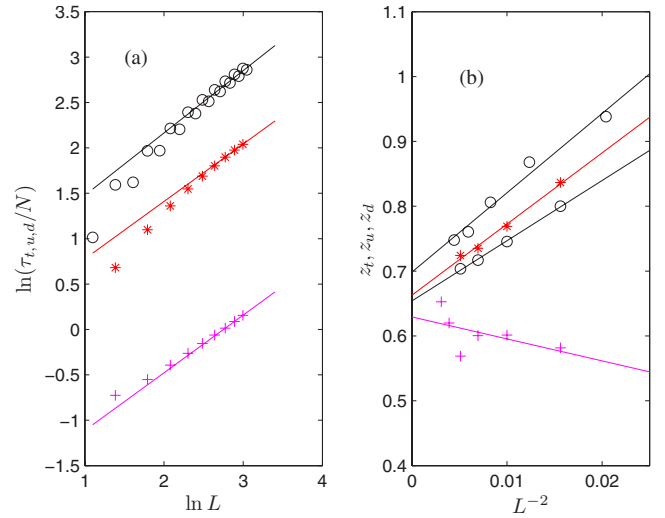

FIG. 5. (Color online) (a) Tunneling times τ_t ($\bigcirc$), τ_u (+), and τ_d (*) as a function of system size L for the Metropolis *et al.* dynamics in a flat energy histogram ensemble obtained from the matrix $T(M;M')$. The fitted straight lines were obtained neglecting data for $L<15$ and have slopes $z_t=0.69$, $z_u=0.64$, and $z_d=0.63$, respectively. In (b) we plot the corresponding local slopes as a function of L^{-2}. For the z_t estimates, even and odd system sides were treated separately. The infinite-size extrapolations are $z_t=0.70(2)$ and 0.65(1) for odd and even system sides, respectively, $z_u=0.63(3)$, and $z_d=0.66(1)$.

$T(M;M')$. The slopes of the fitted straight lines give $z_t=0.69$, $z_u=0.64$, and $z_d=0.63$. The result for z_t can be compared with the value 0.78 reported in Ref. [33] and the value 0.743(7) reported in Ref. [21] by measuring average times for energy excursions. An exponent $z_u=0.6$, also obtained from Monte Carlo estimates of energy tunneling times was previously reported [34] in very good agreement with our result. In Fig. 5(b) we make infinite-size extrapolations giv-
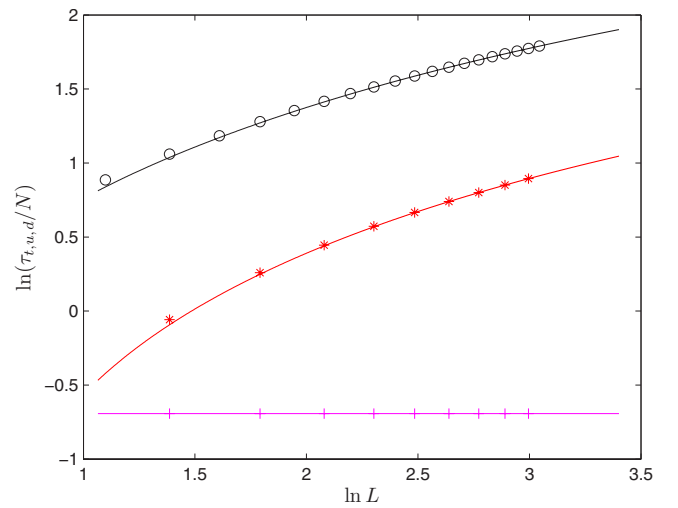

FIG. 6. (Color online) (a) Tunneling times τ_t ($\bigcirc$), τ_u (+), and τ_d (*) as a function of system size L for the Metropolis *et al.* dynamics in a flat magnetization histogram ensemble obtained from the matrix $T(M;M')$. The lines are the analytical asymptotic results given in the text.

TABLE II. Summary of the values obtained for each dynamics of the relaxation time dynamical exponent from magnetization projection, z_M, and energy projection, z_E, and magnetization tunneling exponents z_u, z_d, and z_t obtained from magnetization projection (see text for details).

Dynamics	Relaxation time exponents		Magnetization tunneling exponents		
	z_M	z_E	z_u	z_d	z_t
Critical Glauber	1.99(2)	0(log)			
Critical Metropolis	2.01(1)	0(log)			
Flat E—M	2.08(1)	2.07(1)	0.14(2)	2.08(1)	2.11(1)
Flat E	2.68(3)	1.99(2)–2.07(3)	0.63(3)	0.66(1)	0.65(1)–0.70(2)
Flat M	1.9995(5)	2.002(1)	0	0(log)	0(log)

ing $z_t = 0.70(2)$ and $0.65(1)$ for odd and even system sides, respectively, $z_u = 0.63(3)$, and $z_d = 0.66(1)$.

Finally, we consider the Metropolis *et al.* dynamics for the flat magnetization histogram ensemble. For this case it is possible to compute analytically the tunneling times from the recursion relations given above, Eqs. (23) and (24), and the knowledge of the matrix $T(M; M')$. The analytical results are $\tau_u = N/2$, $\tau_t = (N+1)H(N/2)$, and $\tau_d = \frac{1}{2}[(N+1)H(N/2) - N]$ where $H(n) = \sum_{k=1}^{n} 1/k$ is the harmonic number. Using the known asymptotic result, for large n, $H(n) \sim \ln n + \gamma$ where $\gamma = 0.577\,215\,664\,9\ldots$ is the Euler constant, we have asymptotic expressions for the tunneling times that predict $\tau_t/N \sim \tau_d/N \sim \ln N$, and the tunneling exponents are $z_t = z_d = z_u = 0$. In Fig. 6(a) we compare the numerical results for the tunneling times τ_t, τ_u, and τ_d with the analytical results. Note that, because of the logarithmic dependence of τ_t and τ_u, the estimates for the exponents z_t and z_d that we could obtain for the slopes of the data shown in Fig. 6(a) give effective values around 0.35 that would slowly approach zero only if larger systems were considered.

From the three multicanonical ensembles studied, we see that the flat magnetization ensemble is the one with smaller tunneling exponents and relaxation time exponent. Recently, it was shown that it is possible to optimize the ensemble in multicanonical simulations such that the tunneling exponent z_t is also reduced to zero [33,35].

VI. CONCLUDING REMARKS

We have shown that projected dynamics in the magnetization space is a reasonably good approximation to the full state space single-spin-flip dynamics studied in this work: canonical ensemble Glauber and Metropolis *et al.* dynamics and three multicanonical ensemble dynamics with flat energy-magnetization, flat energy, and flat magnetization histograms. In Table II we have summarized our infinite-size extrapolations of the exponents for the relaxation time and for the magnetization tunneling times. The energy-projected dynamics is generally the worse approximation, being unable to preserve the power-law size increase of the relaxation time for the critical canonical ensemble dynamics. From all the studied dynamics, only the flat energy histogram dynamics show a z exponent clearly larger than 2 and near 2.7. For the case of the flat magnetization histogram, the projection in the magnetization space is exact, and it is possible to obtain analytical results for the tunneling times predicting a zero value for the exponents z_t, z_d, and z_u. The tunneling exponents z_t (and z_d) for the energy and magnetization flat histogram ensemble are much bigger, $z_t = z_d \sim 2$, and larger than the exponent $z_u = 0.14$. For the flat energy histogram dynamics, these three exponents are not very different and the estimates fall between the values $z_u \sim 0.63$ and $z_t \sim 0.70$ for odd system sides. These results were obtained from the tunneling properties of the projected dynamics in the magnetization space which were found to be in rough agreement with those obtained by independent methods for excursions in the energy space for the flat energy multicanonical ensemble.

Finally, the results show that the evaluation of the relative performance of single-spin-flip dynamics in Ising-like models can be done very efficiently by studying the projected dynamics in the magnetization space: the approximation gives reasonably accurate dynamic exponents, any arbitrary single-spin-flip dynamics can be studied from Monte Carlo estimations of $T_\infty(E, M; E', M')$ for several system sizes in the energy-magnetization space, and the large dimensional reduction achieved by the projection in the magnetization space allows the application of matrix diagonalization techniques for bigger system sizes. Furthermore, the application of projection methods to cluster dynamics in Ising models and other models, including continuous spin models [36,37], projected along their slowest mode may be of considerable interest.

[1] P. C. Hohenberg and B. I. Halperin, Rev. Mod. Phys. **49**, 435 (1977).

[2] A. D. Sokal, in *Functional Integration: Basics and Applications*, edited by C. DeWitt-Morette, P. Cartier, and A. Folacci (Plenum, New York, 1997), p. 131.

[3] M. P. Nightingale and H. W. J. Blöte, Phys. Rev. Lett. **76**, 4548 (1996).

[4] M. P. Nightingale and H. W. J. Blöte, Phys. Rev. B **62**, 1089 (2000).

[5] R. H. Swendsen and J. S. Wang, Phys. Rev. Lett. **58**, 86 (1987).

[6] U. Wolff, Phys. Rev. Lett. **62**, 361 (1989).

[7] B. A. Berg and T. Neuhaus, Phys. Rev. Lett. **68**, 9 (1992).

[8] J. Lee, Phys. Rev. Lett. **71**, 211 (1993).

[9] G. Bhanot, R. Salvador, S. Black, P. Carter, and R. Toral, Phys. Rev. Lett. **59**, 803 (1987).

[10] J. Lee, M. A. Novotny, and P. A. Rikvold, Phys. Rev. E **52**, 356 (1995).

[11] I. Shteto, J. Linares, and F. Varret, Phys. Rev. E **56**, 5128 (1997).

[12] I. Shteto, K. Boukheddaden, and F. Varret, Phys. Rev. E **60**, 5139 (1999).

[13] M. Kolesik, M. A. Novotny, and P. A. Rikvold, Phys. Rev. Lett. **80**, 3384 (1998).

[14] M. A. Novotny, in *Annual Reviews of Computational Physics IX*, edited by D. Stauffer (World Scientific, Singapore, 2001), p. 153.

[15] M. Kolesik, M. A. Novotny, P. A. Rikvold, and D. M. Townsley, in *Computer Simulation Studies in Condensed Matter Physics X*, edited by D. P. Landau, K. K. Mon, and H. B. Schüttler (Springer, Berlin, 1998), p. 246.

[16] J. G. Kemeny and J. L. Snell, *Finite Markov Chains* (Springer, New York, 1976).

[17] N. Metropolis, A. W. Rosenbluth, M. N. Rosenbluth, A. H. Teller, and E. Teller, J. Chem. Phys. **21**, 1087 (1958).

[18] R. J. Glauber, J. Math. Phys. **4**, 294 (1963).

[19] J. S. Wang, T. K. Tay, and R. H. Swendsen, Phys. Rev. Lett. **82**, 476 (1999).

[20] J. S. Wang and R. H. Swendsen, J. Stat. Phys. **106**, 245 (2002).

[21] P. Dayal, S. Trebst, S. Wessel, D. Würtz, M. Troyer, S. Sabhapandit, and S. N. Coppersmith, Phys. Rev. Lett. **92**, 097201 (2004).

[22] M. D. Costa, J. V. Lopes, and J. M. B. Lopes dos Santos, Europhys. Lett. **72**, 802 (2005).

[23] P. D. Beale, Phys. Rev. Lett. **76**, 78 (1996).

[24] A. R. Lima, P. M. C. de Oliveira, and T. J. P. Penna, Solid State Commun. **114**, 447 (2000).

[25] P. M. C. de Oliveira, T. J. P. Penna, and H. J. Herrmann, Braz. J. Phys. **26**, 677 (1996).

[26] P. M. C. de Oliveira, Braz. J. Phys. **30**, 195 (2000).

[27] P. M. C. de Oliveira, Eur. Phys. J. B **6**, 111 (1998).

[28] A. Bortz, M. H. Kalos, and J. L. Lebowitz, J. Comput. Phys. **17**, 10 (1975).

[29] W. H. Press *et al.*, *Numerical Recipes in Fortran 77: The Art of Scientific Computing*, 2nd ed. (Cambridge University Press, New York, 1992), Vol. 1.

[30] E. Domany, Phys. Rev. Lett. **52**, 871 (1984).

[31] M. Arjunwadkara, M. Fasnacht, J. B. Kadane, and R. H. Swendsen, Physica A **323**, 487 (1995).

[32] M. L. Guerra and J. D. Muñoz, Int. J. Mod. Phys. C **15**, 471 (2004).

[33] J. Viana Lopes, M. D. Costa, J. M. B. Lopes dos Santos, and R. Toral, Phys. Rev. E **74**, 046702 (2006).

[34] J. V. Lopes, Ph.D. thesis, Universidade do Porto, 2006.

[35] S. Trebst, D. A. Huse, and M. Troyer, Phys. Rev. E **70**, 046701 (2004).

[36] J. D. Munoz and H. J. Herrmann, Comput. Phys. Commun. **122**, 13 (1999).

[37] S. J. Mitchell, M. A. Novotny, and J. D. Munoz, Int. J. Mod. Phys. C **10**, 1503 (1999).